Journal of Solid State Chemistry **145,** 549–556 (1999)
Article ID jssc.1999.8216, available online at http://www.idealibrary.com on IDEAL®

The Layered Intercalation Compounds $Li(Mn_{1-y}Co_y)O_2$: Positive Electrode Materials for Lithium–Ion Batteries

A. Robert Armstrong, Alastair D. Robertson, Robert Gitzendanner, and Peter G. Bruce[1]

School of Chemistry, University of St. Andrews, Purdie Building, St. Andrews, Fife KY16 9ST, United Kingdom

Received September 2, 1998; in revised form February 10, 1999; accepted February 11, 1999

The layered intercalation compounds $Li(Mn_{1-y}Co_y)O_2$; $0 \leq y \leq 0.5$ cannot be prepared by conventional solid state reaction but have been synthesized using a solution-based route coupled with ion exchange. A continuous range of solid solutions with rhombohedral symmetry exists for $0.1 \leq y \leq 0.5$. Consideration of transition metal to oxygen bond lengths indicates that Mn^{3+} is replaced by cobalt in the trivalent state. Localized high spin Mn^{3+} ($3d^4$) induces a cooperative Jahn–Teller distortion in layered $LiMnO_2$, lowering the symmetry from rhombohedral $R\bar{3}m$ to monoclinic ($C2/m$). Substitution of as little as 10% Mn by Co is sufficient to suppress the distortion in $Li_{0.9}(Mn_{0.9}Co_{0.1})O_2$, whereas half the Li must be extracted from $LiMnO_2$ to achieve a single undistorted rhombohedral phase. On removing and reinserting Li in $LiMnO_2$ only half the quantity of Li (equivalent to a specific charge of 130 $mAhg^{-1}$) may be reinserted on the first cycle; this substantial drop in capacity is eliminated with only 10% Co substitution. The latter material can sustain a large capacity on cycling (200 $mAhg^{-1}$). Higher Co contents have somewhat lower capacities but fade less at higher cycle numbers. The marked improvement in capacity retention of the Co-doped materials compared with pure $LiMnO_2$ may be related in part to the absence of the Jahn–Teller distortion. Electrochemical data indicate conversion to a spinel-like structure on cycling. Such conversion is progressively slower with increasing Co content. Cycling of this spinel-like material is significantly better than Co-doped spinel of the same composition. These materials are of interest as electrodes in rechargeable lithium batteries.

INTRODUCTION

Low dimensional solids have been a long standing interest of Peter Day because dimensional confinement induces fascinating and often unique properties in the compounds that adopt such structures. This is true not just for magnetic and electronic properties but also in the field of intercalation chemistry. The ability to insert and subsequently remove guest species between the van der Waal's bonded layers of transition metal sulphides, selenides, or tellurides, such as TiS_2, received a great deal of attention between the 1950s and 1970s and this interest continues today (1). In more recent times, interest in the intercalation chemistry of layered oxides has grown enormously (2). These compounds are both interesting and challenging to solid state chemists because the much weaker van der Waal's forces between oxide layers compared with the chalcogenides means that the oxides demonstrate little propensity to adopt layered structures in the absence of guest species. This is highlighted by the fact that only recently has it been possible to prepare layered CoO_2 and NiO_2 by removing lithium from the well-known layered compounds $LiCoO_2$ and $LiNiO_2$ under vigorously oxidizing conditions in an electrochemical cell (3, 4).

A strong technological force driving interest in layered lithium transition metal oxides is their use as positive electrodes in rechargeable lithium–ion batteries (2). Launched in the early 1990s (5), this revolutionary device represents one of the fastest growing high technology products with production doubling each layer. The unique advantage of these cells is that they can store up to three times the energy compared with conventional batteries of the same size and weight. Lithium–ion batteries are already transforming the size of mobile telephones and lap–top computers and will make possible significant advances in electric vehicles and many other applications in the next decade. The cell is an elegant example of solid state chemistry (2). On charging, lithium is removed from the $LiCoO_2$ positive electrode then reinserted on discharge (6). The rate of these intercalation processes determines directly the rate at which the battery may be charged and discharged. The voltage of the cell depends on the chemical potential of lithium in the host, i.e., on the site energy for the guest lithium–ions and the electronic Fermi level. The ability to store charge is a function of the amount of lithium which may be removed and reinserted and the reversibility of this process determines the cyclability of the cell (7–8).

Although $LiCoO_2$ has formed the basis of the positive electrodes in all commercial lithium–ion cells to date, the

[1] To whom correspondence should be addressed.

0022-4596/99 $30.00

relatively high cost and toxicity of this material means that substantial advances in lithium–ion battery technology demand its replacement. A consideration of all the factors required for operation as a positive electrode leads to the conclusion that compounds based on manganese oxides, which are significantly cheaper and less toxic than the cobalt oxides, are particularly attractive (9). The spinel, $LiMn_2O_4$, was found to act as an intercalation host for lithium in the early 1980s (10–12). Further development has resulted in this compound being introduced as a replacement for $LiCoO_2$ in second generation lithium–ion batteries (13–17). Unfortunately only 0.5 Li per Mn can be removed and reinserted reversibly in the spinel host corresponding to the storage of 110 $mAhg^{-1}$ of charge. This is already somewhat less than the practical capacity of $LiCoO_2$ at 130 $mAhg^{-1}$ which is itself much less than this compound's theoretical capacity of 273 $mAhg^{-1}$. The goal is to synthesize compounds that combine low cost and toxicity with the ability to store reversibly charge greater than 130 $mAhg^{-1}$.

The success of $LiCoO_2$ encouraged our interest in layered $LiMnO_2$ as an intercalation host for use in lithium–ion batteries on the basis that the layered structure should lead to facile lithium transport while replacement of cobalt by manganese provides cheaper and less toxic materials. Whereas the majority of layered transition metal oxides may be prepared by conventional solid state synthesis, this is not the case for $LiMnO_2$. The similarity of the Li^+ and Mn^{3+} ionic radii does not favour the formation of a true layered structure. Recently we reported the first synthesis of layered $LiMnO_2$ (18, 19). This was achieved by preparing $NaMnO_2$, which does adopt a layered structure. The low dimensionally is promoted by the very different ionic radii and bonding of Na^+ and Mn^{3+}. The sodium ions may then be ion-exchanged for lithium by refluxing in a high boiling non aqueous solvent such as hexanol. This provides sufficiently vigorous conditions for complete exchange whilst preserving the layered structure. Recently layered $LiMnO_2$ has been prepared hydrothermally (20). When incorporated in an electrochemical cell, a significant amount of lithium may be removed corresponding to a specific charge capacity of 220 $mAhg^{-1}$. However, only around half of this may be reinserted on the subsequent discharge, rendering this otherwise interesting compound of less technological significance. We are exploring modifications of layered $LiMnO_2$, in particular solid solution formation, anticipating that this may improve the stability of the structure and hence its ability to sustain repeated lithium intercalation–deintercalation.

In this paper we report on the formation of solid solutions between $LiMnO_2$ and $LiCoO_2$. The latter compound can sustain many charge–discharge cycles. It was hoped that by introducing some cobalt into $LiMnO_2$ a balance could be obtained between the advantageous cost and toxicity of a manganese-rich material with the excellent cycling performance of the cobalt-rich oxide. A preliminary note has already appeared dealing only with the substitution of 10% of the manganese by cobalt (21). Here we describe the synthesis, structural characterization, and electrochemical investigation of a range of solid solutions $Li(Mn_{1-y}Co_y)O_2$; $0 \leq y \leq 0.5$. Compositions with more than 50% Co are unlikely to be of interest from the viewpoint of cost and toxicity.

EXPERIMENTAL

The synthesis of $LiMn_{1-y}Co_yO_2$ was achieved via initial preparation of the corresponding sodium-containing phase followed by ion exchange to replace the sodium by lithium. A solution route was used to prepare the parent compound. An aqueous solution of Na_2CO_3 (Aldrich 99% +) was added to a solution containing managanese (II) acetate, $Mn(CH_3COO)_2 \cdot 4H_2O$ (Aldrich, 99% +), and cobalt (II) acetate, $Co(CH_3COO)_2 \cdot 4H_2O$ (Aldrich 90% +) in the appropriate stoichiometric ratio. The resulting precipitate was dried by rotary evaporation and fired for several hours at 250°C in air to decompose the organic material. The product was ground using a mortar and pestle and fired in air at temperatures ranging from 670 to 800°C for 1 h before quenching to room temperature. Lower temperatures were emplyed for lower cobalt doping levels, rising to 800°C for 50% Co. Phase purity was verified by powder X-ray diffraction using a Philips X'Pert PW3020 diffractometer operating with Bragg–Brentano geometry and Cu$K\alpha$ radiation. An analyzing graphite monochromator was employed to reduce fluorescence at the detector. Ion exchange experiments, to replace the sodium by lithium, employed the same route as was used in the preparation of layered $LiMnO_2$, i.e., reflux in *n*-hexanol at 150°C with a 10-fold excess of LiBr for 6–8 h (18). After cooling, the material was filtered under suction, washed with alcohol, and dried. Lithium concentrations were determined by flame emission analysis.

The structures of these materials were characterized using neutron diffraction. Time-of-flight powder neutron diffraction data were collected on the POLARIS high-intensity, medium-resolution instrument at ISIS, Rutherford Appleton Laboratory (22). Since lithium, manganese, and cobalt are all neutron absorbers the data were corrected for attenuation prior to refinement. The structures were refined by the Rietveld method using the program TF12LS based on the Cambridge Crystallographic Subroutine Library (23, 24). Neutron scattering lengths of -0.19, -0.373, 0.278, and 0.5803 (all $\times 10^{-12}$ cm) were assigned to Li, Mn, Co, and O, respectively (25).

Electrodes were prepared by forming a composite between the $LiMn_{1-y}Co_yO_2$ cathode material, super S carbon, and Kynar Flex 2801 binder (a copolymer based on PVDF) in the weight ratios 85 : 10 : 5. The electrodes were

cast on to Al foil. Galvanostatic cycling and cyclic voltammetry were performed in three electrode cells. The electrolyte consisted of a 1 M solution of $LiPF_6$ dissolved in 2:1 EC:DMC, and the counter and reference electrodes were fashioned from lithium metal. The electrochemical experiments were carried out using a computer controlled Biologic Macpile multichannel instrument.

RESULTS AND DISCUSSION

The $Li(Mn_{1-y}Co_y)O_2$ compounds in the range $0 \leq y \leq 0.5$ could not be prepared by conventional solid state reaction necessitating the use of the ion exchange route described in the Experimental Section.

The Compounds

Five compositions were examined by powder neutron diffraction, $Li_xMn_{0.9}Co_{0.1}O_2$, $Li_xMn_{0.8}Co_{0.2}O_2$, $Li_xMn_{0.7}Co_{0.3}O_2$, $Li_xMn_{0.6}Co_{0.4}O_2$, and $Li_xMn_{0.5}Co_{0.5}O_2$. In all cases the data could be indexed on a rhombohedral cell with systematic absences consistent with space group $R\bar{3}m$ (no. 166). The layered α-$NaFeO_2$ structure of $LiCoO_2$ ($R\bar{3}m$) was used as the starting model for refinement by the Rietveld method (26). In this structure the oxide ions adopt a cubic close packed arrangement. The sheets of octahedral sites between layers of the oxide ions are occupied alternately by transition metal and lithium–ions. Mn and Co were placed on a 3a octahedral sites within the transition metal layers. Their occupancies were allowed to vary with the sum constrained to equal unity. Li^+ ions were located on the 3b octahedral sites in the lithium layers with the occupancy of these sites being permitted to vary without limit. For all compositions, the profile fit was good as exemplified by the data for $Li_xMn_{0.9}Co_{0.1}O_2$, Fig. 1. The crystallographic data for this compound are presented in Table 1 and correspond to a χ^2 of 3.7 for 3121 observations and 22 variables. The weighted profile R factor was 2.1 with an expected R of 1.1. The refined Mn/Co ratios for the compositions studied are presented in Fig. 2 from which it may be seen that these are in good agreement with the values expected from the synthesis. For most of the compositions the Mn content is higher, to a small degree, than expected. The refined lithium content was found to be less than 1 for all samples with the values varying from 0.81 (10% Co) to 0.71 (50% Co). The atomic emission analysis, used to determine the lithium contents, agreed well with the values obtained from refinement based on the neutron data; for example, the refined content for 10% substitution of manganese by cobalt was found to be 0.81 (5) and the figure from emission analysis was 0.78 (2). The reason for the slight Li deficiency in all samples is that the sodium phase formed by high temperature solid state reaction is deficient in Na. As stated in the experimental section, higher firing temperatures were required for higher Co contents leading to a greater loss of sodium. There is negligible residue of sodium (i.e. $\ll 1\%$) in the Li compounds.

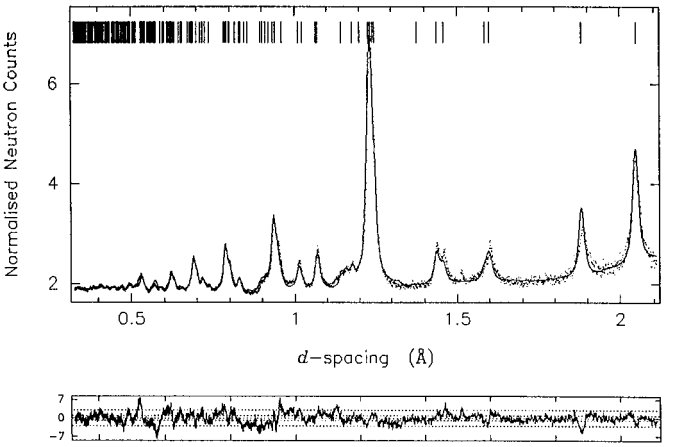

FIG. 1. Powder neutron diffraction profile for the nominal composition $Li_x(Mn_{0.9}Co_{0.1})O_2$. Dots represent the observed data, solid line represents the best fit, and the lower curve corresponds to the difference between the observed and calculated profiles. Verticle lines indicate the positions of reflections.

The variation of the lattice parameters with cobalt content is presented in Fig. 3. The c-axis rises marginally to a peak around 30% substitution by cobalt. The more important variation occurs in the a parameter which decreases from a value of 2.873(1) Å at 10% cobalt substitution to 2.825(1) Å at 50% Co. The a lattice parameter departs only marginally from Vegard's Law, indicated by a slight upward curvature of a with increasing Co content. The c/a ratios are reported in Table 2. For the 10% substituted material the c/a ratio is 5.006 and increases with increasing cobalt content. A c/a ratio of 4.9 in rhombohedral symmetry is equivalent to a cubic unit cell. It has been shown previously that a cubic spinel structure and a layered rhombohedral structure with such a c/a ratio are indistinguishable with diffraction techniques (27, 28). It is clear from the magnitude of the c/a ratios reported here that the layered compound is the dominant phase at all cobalt contents rather than spinel. There is little evidence of spinel being present even as a second phase in the neutron data at any of the compositions studied.

TABLE 1
Crystallographic Data for $Li_xMn_{0.9}Co_{0.1}O_2$

Atom	Wcykoff symbol	x/a	y/a	z/c	B_{iso}	Occupancy
Li	3b	0.0	0.0	0.5	2.2(2)	0.81(5)
Mn/Co	3a	0.0	0.0	0.0	0.39(6)	0.93/0.07(1)
O	6c	0.0	0.0	0.26129(11)	0.71(3)	1

Note. Space group $R\bar{3}m$ (no. 166). $a = 2.8734$ (2) Å, $c = 14.3843$ (12) Å. $\chi^2 = 3.7$, R_{exp} 1.1%; $R_{wp} = 2.1\%$; $R_p = 2.1\%$; $R_I = 6.0\%$.

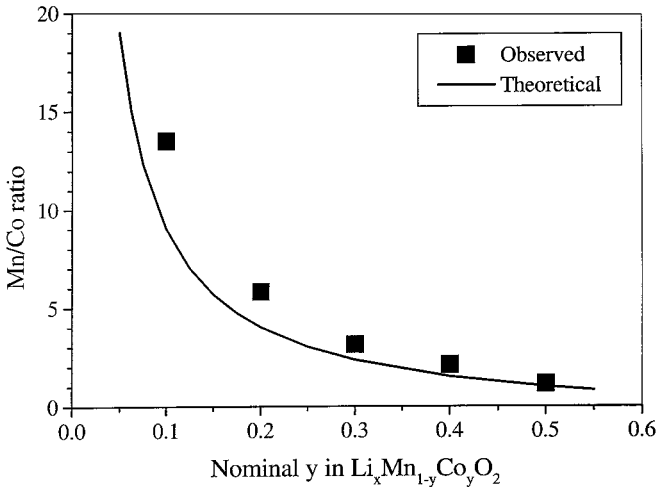

FIG. 2. Variation of the Mn/Co ratio with nominal Co content. The solid line corresponds to the ratio expected on the basis of the nominal Co content and the solid squares to the ratio obtained from the neutron diffraction data.

Co could enter the layered $LiMnO_2$ structure as either Co^{3+} or Co^{2+} although the former is more likely based on the trivalent oxidation state in layered $LiCoO_2$. Assuming Mn^{3+} is replaced by Co^{3+}, a contraction of the *a*-axis and, more particularly, the average (Mn/Co)–O bond is anticipated because of the smaller ionic radius of low spin Co^{3+} (0.545 Å) compared with high spin Mn^{3+} (0.645 Å) (radii from Ref. 29). A plot comparing the expected contraction of the (Mn/Co)–O bond with the observed variation is shown in Fig. 4. The expected contraction is based on the average Mn^{3+}/Co^{3+} radius calculated from the data of Shannon (29). Since pure $LiMnO_2$ is monoclinic and hence the six Mn–O distances are not all equivalent, the bond length

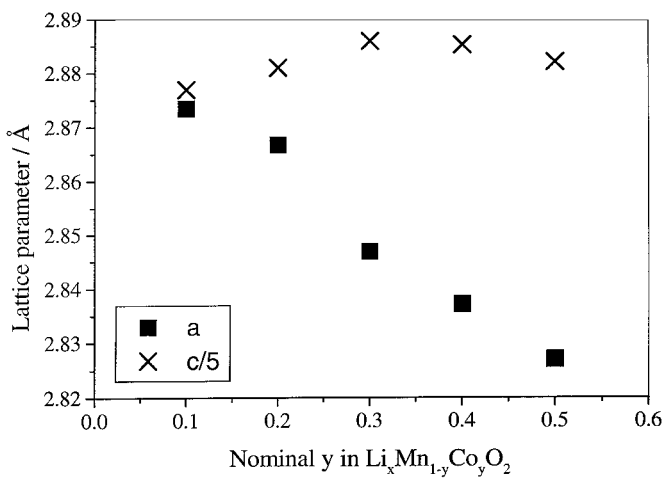

FIG. 3. Variation of the *a* and *c* lattice parameters as a function of Co content.

TABLE 2
***c/a* Ratios for Several Compositions in the Solid Solution Series $Li_xMn_{1-y}Co_yO_2$, as Determined by Powder Neutron Diffraction**

Nominal Co content	*c/a* Ratio
0.1	5.006
0.2	5.025
0.3	5.068
0.4	5.085
0.5	5.097

contractions use the nominal 10% Co substituted material as the base line. Replacement of Mn^{3+} by Co^{2+} requires introduction of an equivalent amount of Mn^{4+}. The average ionic radius of high spin Co^{2+} (0.745 Å) and Mn^{4+} (0.53 Å) is 0.64 Å which is very similar to that of high spin Mn^{3+}. The much smaller variation in the average transition metal to oxygen bond length (anticipated for substitution by Co^{2+}) is not consistent with the observed bond length changes, Fig. 4. This points to substitution by Co^{3+} rather than Co^{2+} as the mechanism of solid solution formation. The lithium deficiency introduces some Mn^{4+}; however, this varies relatively little with Co content and does not significantly influence the results. Also the theoretical bond length calculation assumes a linear variation. This is reasonable given the variation of the *a* lattice parameter with Co content.

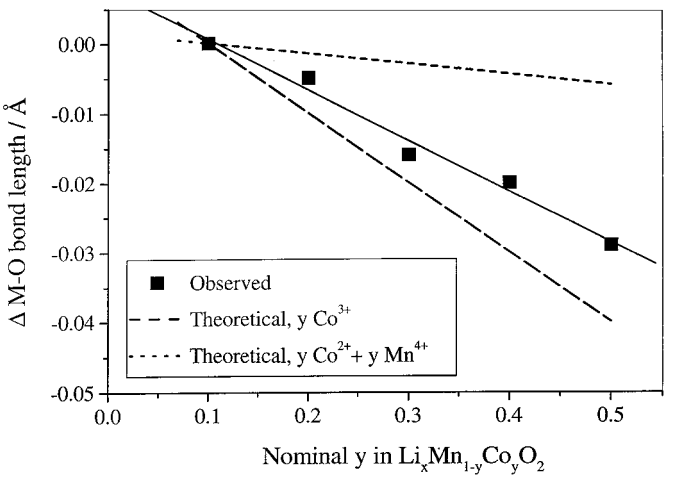

FIG. 4. Plot of the average (Mn/Co)–O bond contraction as a function of the nominal Co content. The squares represent the observed bond length contraction from neutron diffraction. The dashed line corresponds to the bond length contraction anticipated from the change in the average ionic radius as Mn^{3+} is replaced by Co^{3+}. The dotted line represents the expected bond length contraction based on replacing Mn^{3+} by Co^{2+} which generates an equivalent amount of Mn^{4+}. The average ionic radii were calculated based on the data of Shannon (29).

The absence of a monoclinic distortion at low cobalt content is particularly noteworthy. In the case of $LiMnO_2$ the localized high spin d^4 configuration of the Mn^{3+} ion induces a cooperative Jahn–Teller distortion of the octahedral sites lowering the crystal symmetry from rhombohedral ($R\bar{3}m$) to monoclinic ($C2/m$) (18). On removing half the lithium, 50% of the Mn^{3+} ions are oxidized to Mn^{4+}. When the occupancy of the octahedral sites by Mn^{3+} has been reduced to one half, the cooperative Jahn–Teller distortion does not occur and a single undistorted phase of rhombohedral symmetry is obtained. Between $x = 0.5$ and 1 in Li_xMnO_2, there exists a two phase mixture of rhombohedral, $Li_{0.5}MnO_2$, and monoclinic, $LiMnO_2$ (30). In contrast, by replacing only 10% of the Mn^{3+} ions with Co in $Li_{0.8}Mn_{0.9}Co_{0.1}O_2$ the cooperative distortion disappears. We have also inserted lithium into this compound and find that for compositions approaching $Li_{0.9}Mn_{0.9}Co_{0.1}O_2$ there is little evidence of a Jahn–Teller distortion in the powder neutron diffraction data; only a single rhombohedral phase is observed. If cobalt is in the trivalent state then 80% of the transition metal sites are occupied by Mn^{3+}. We may speculate on why the Jahn–Teller distortion and consequent two phase mixture observed for Li_xMnO_2, $0.5 < x < 1$ is suppressed by modest Co doping. In the pure Li_xMnO_2 compounds, the e_g electron on Mn^{3+} is free to move between Mn^{3+} and Mn^{4+} by small polaron hopping. The Li^+ ions are also mobile. Clustering of electrons leads to Mn^{3+} rich regions, and as a result a relatively unhindered cooperative Jahn–Teller distortion, is possible. Reduction in the Mn^{3+} content by Co^{3+} doping rather than generating Mn^{4+} by lithium extraction inhibits such clustering, since any Mn^{3+} and Li^+ rich regions that form will also contain the Jahn–Teller inactive Co^{3+}, the distribution of which is frozen into the structure on synthesis. Hence formation of a 2-phase Jahn–Teller distortion is more difficult. It is interesting to compare Co-doped $LiMnO_2$ with the isostructural layered $LiNiO_2$ compound. $LiNiO_2$ contains low spin Ni^{3+}, $3d^7$ ($t_{2g}^6 e_g^1$) and as a result is similar to the manganese phase with one electron in the e_g orbitals. Despite this, $LiNiO_2$ ($R\bar{3}m$) does not exhibit a cooperative Jahn–Teller distortion. Replacement of Mn^{3+} by Co^{3+} results in a shortening of the (Mn/Co)–O bond approaching Ni–O in $LiNiO_2$ with a consequent perturbation of the electronic structure toward that of $LiNiO_2$. It may be that the absence of a cooperative distortion in $Li_xMn_{1-y}Co_yO_2$ and $LiNiO_2$ has a similar origin. It may also be noted that 5% of vacancies on the transition metal sites of $Li_{0.8}Mn_{0.9}Co_{0.1}O_2$ is sufficient to reduce the Mn^{3+} content to 50%. This level of vacancies is comparable to the accuracy of the site occupancies from neutron diffraction. All such ideas on the absence of a Jahn–Teller distortion remain speculature until further studies are complete.

Summarizing this section, the structural data indicate successful preparation of a range of solid solutions with up to 50% of the manganese replaced by cobalt in layered $LiMnO_2$.

The Electrochemistry and Cell Performance

The purpose of investigating cobalt doping in the layered compound $LiMnO_2$ was to establish if such a process could enhance the ability of this compound to sustain the reversible removal and reinsertion of lithium. The capacity of the pure $LiMnO_2$ compound is shown in Fig. 5 which also contains cycling data for the compound with 10, 20, 30, and 50% Mn replaced by Co. The cycling was carried out at a current density of 0.1 $mAcm^{-2}$ and between potential limits of 2.6 and 4.8 V. The data demonstrate that as little as 10% Co is required to improve the cycling performance substantially and eliminate the large loss of capacity on the first cycle encountered with $LiMnO_2$. The 10% substituted material yields an initial discharge capacity on the first cycle of 210 $mAhg^{-1}$ (following a charge of 212 $mAhg^{-1}$) falling, after some 20 cycles, to 200 $mAhg^{-1}$. Increasing the cobalt content to 20% reduces the initial discharge capacity compared with the 10% material; however, after a modest rise within the first three cycles, the capacity varies little with cycle number. Above 30 cycles the values are only marginally lower than the 10% material. For Co contents greater than 30% there is an even lower initial discharge capacity which declines further on cycling.

The load curves collected for materials substituted with 10, 20, and 30% cobalt at a current density of 0.1 $mAcm^{-2}$ are shown in Fig. 6. In all cases it is clear that the first charge is markedly different from subsequent charges and that after several cycles the discharge curves exhibit the formation of a plateau in the 3 V region. A plateau also develops in the 4 V region within the first few cycles for the manganese rich compounds; its development requires more charge–discharge cycles as the cobalt content increases. For the

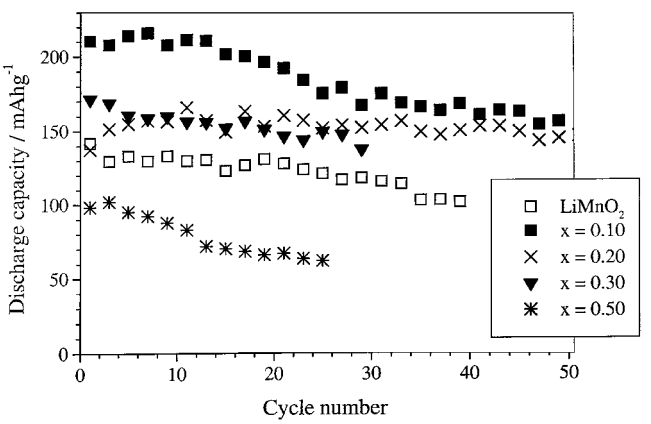

FIG. 5. Discharge capacity as a function of cycle number for layered $LiMnO_2$ and $Li_xMn_{1-y}Co_yO_2$ (nominal compositions) at 0.1 $mAcm^{-2}$ and potential limits of 2.6 and 4.8 V.

material with 30% cobalt, plateau formation at 4 V is only just evident after 30 cycles. Although the load curves for the material with 10% cobalt suggest a significant structural change within the first five cycles, it is apparent from Fig. 5 that the capacity fade is insensitive to this structural transformation. The stability of the load curves from cycle 5 to 15 for the materials with 10 and 20% cobalt is in accord with the stable discharge capacities observed for these materials over this range.

In order to shed further light on the intercalation process, incremental capacity plots were derived from the data presented in Fig. 6 for the materials containing 10, 20, and 30% cobalt as well as for cobalt doped spinel $Li[Mn_{1.8}Co_{0.2}]O_4$ which has the same Mn:Co:O stoichiometry as the 10% substituted layered compound and is therefore directly comparable with it. The spinel was prepared following our previously reported method in which Li_2CO_3 is mixed with manganese and cobalt acetates in water; the mixture is then dried, prefired to decompose the organic material, and heated at 600°C (16, 31). The incremental capacity plots corresponding to the third cycle are shown in Fig. 7a. The most striking feature is the similarity between the data for the layered compounds with cobalt contents up to 20% and Co-doped spinel in the 4 V region. For the layered compounds two pairs of redox peaks are evident, one at 4 and the other at 4.1 V, exactly coincident with the peaks from the spinel phase. For the 10% doped material there is also considerable similarity between the redox peaks for the layered and spinel compounds at 3 V. These data suggest that the Mn/Co layered compounds convert significantly to spinel within a few cycles, for cobalt contents up to 20% but that conversion is slower for 20% compared with 10%. The material with 30% cobalt behaves differently. The 4 V peaks normally associated with spinel are not well developed with only the hint of a reduction process at 3.9 V. The incremental capacity data for the 30th cycle are shown in Fig. 7b. Oxidation and reduction peaks between 3.9 and 4 V are now more evident in the 30% material. These data indicate that transformation to spinel is relatively facile for layered compounds with a low cobalt content ($< 30\%$) but that above this composition transformation is much slower. This is consistent with the fact that $LiCoO_2$ remains layered on cycling whereas layered $LiMnO_2$ converts to spinel by displacement of one quarter of the manganese ions from the transition metal layers into the octahedral sites in the lithium layers. The stability of low spin Co^{3+} in an octahedral site compared with its stability in a tetrahedral oxygen environment, through which the cobalt ion would have to pass in order to migrate from the transition metal layers into the lithium layers, is at least in part responsible for the greater stability of the layered structure with increasing Co content.

Detailed examination of the incremental capacity plots for layered $Li_xMn_{1-y}Co_yO_2$ reveal that the electrochemistry is complex. Several features exist in addition to the signature for spinel transformation. There is a well-defined peak around 3.7 V on oxidation which shifts slightly with

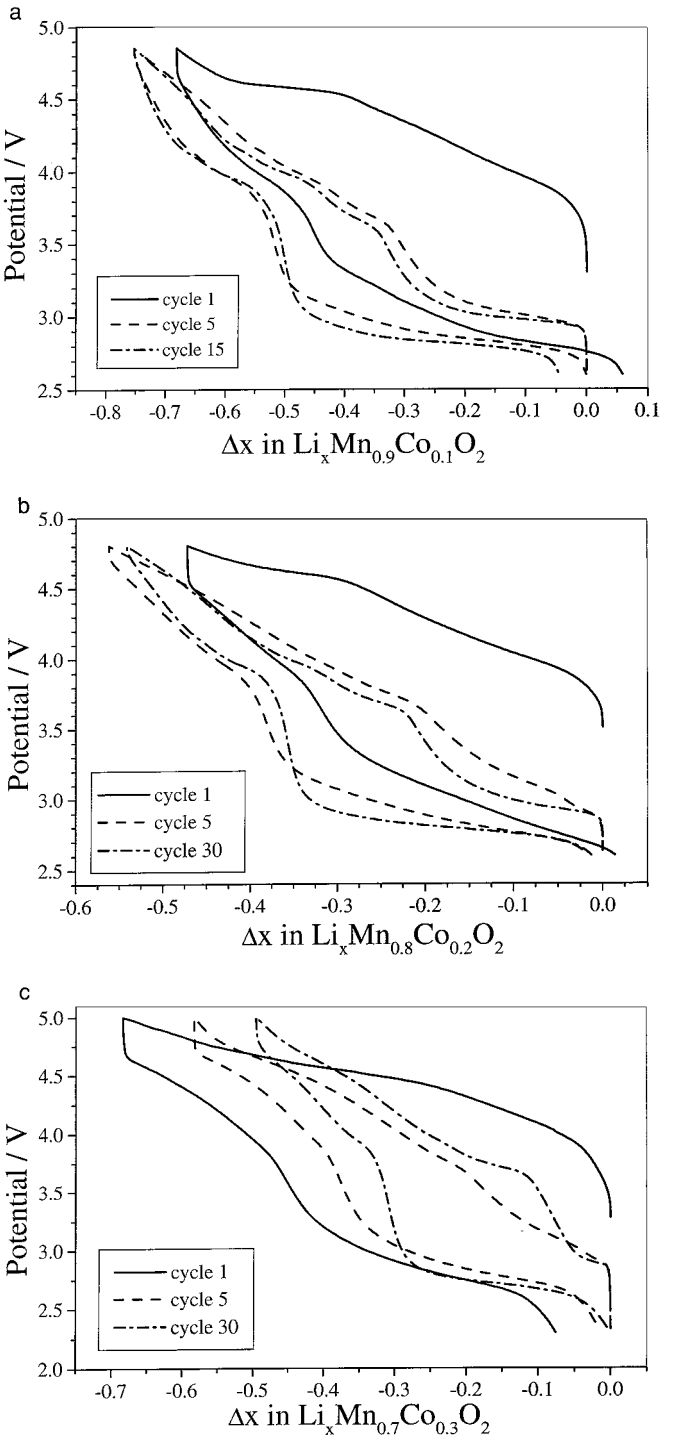

FIG. 6. Load curves for three solid solutions doped with nominal Co contents of (a) 10%, (b) 20%, and (c) 30%. The data were collected at a constant current of 0.1 $mAcm^{-2}$. The change in lithium content during a given cycle is shown on the *x*-axis.

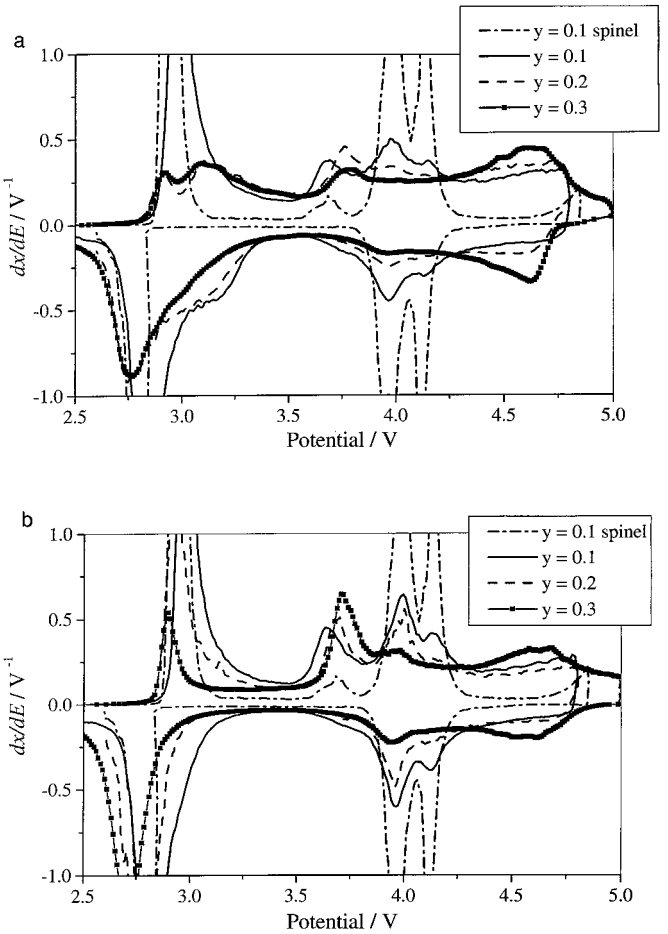

FIG. 7. Incremental capacity plots for $Li(Mn_{1.8}Co_{0.2})O_4$ spinel and the layered compounds of nominal composition $Li_xMn_{1-y}Co_yO_2$ (a) after three cycles and (b) after 30 cycles. Data collected at 0.1 $mAcm^{-2}$.

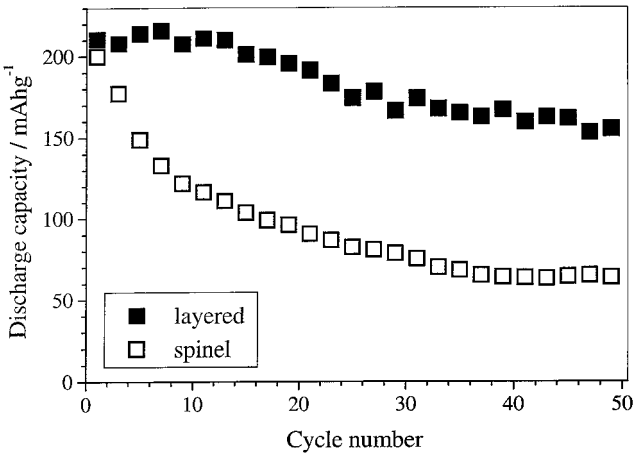

FIG. 8. Discharge capacity as a function of cycle number for layered $Li_xMn_{0.9}Co_{0.1}O_2$ and $Li_2Mn_{1.8}Co_{0.2}O_4$ spinel at 0.1 $mAcm^{-2}$ between 2.6 and 4.8 V.

Co content. This process is also evident in the Co-doped spinel but is absent in $LiMn_2O_4$. The peak appears therefore to be associated with the presence of Co. Gummow, Liles, and Thackeray have noted processes near 3.7 V in low temperature $LiCoO_2$ which has a structure intermediate between normal spinel and high temperature layered $LiCoO_2$ (28). Peaks are also evident for the layered compounds in Fig. 7 at 3.1 and 4.6 V.

It is important to note that conversion of the layered mixed metal systems to spinel results in a material which is distinct from cobalt doped spinel prepared by direct reaction. This is particularly evident in the data presented in Fig. 8 where the capacity fade for $LiMn_{1.8}Co_{0.2}O_4$ spinel is compared with layered $Li_xMn_{0.9}Co_{0.1}O_2$. Although both these compounds, which have the same Mn:Co:O ratios, commence with a discharge capacity $> 200\ mAhg^{-1}$, the capacity fade for the spinel material over the voltage range (2.6 to 4.8 V) is significantly greater than for the spinel material derived from layered $LiMn_{0.9}Co_{0.1}O_2$. It appears that, as in the case of layered $LiMnO_2$, the spinel-like material displays intercalation processes with quite different reversibility compared with the spinel prepared at high temperature.

The results reported here advance our understanding but raise additional questions. Further and extensive studies are already underway to establish the electronic structure of the solid solutions including confirming the oxidation states of the transitional metal ions. Studies are also underway to establish the local structure, answering questions such as the existence of Co clustering and any local Jahn–Teller distortion around Mn^{3+}. These studies should also lead to a better understanding of the absence of a cooperative Jahn–Teller distortion. By combining the electrochemical measurements on cycling with structural studies as a function of Li content and cycle number it will be possible to interpret the additional redox processes evident in Fig. 7.

Although questions remain we have shown that cobalt doping can substantially alter the structural chemistry and electrochemistry of layered $LiMnO_2$, that a small amount of cobalt doping can remove the significant capacity loss occurring on the first cycle, and that higher cobalt levels can significantly suppress the transition to a spinel-like structure.

ACKNOWLEDGMENTS

PGB is indebted to the EU and the EPSRC for financial support.

REFERENCES

1. D. W. Bruce and D. O'Hare, *in* "Inorganic Materials," Wiley, New York, 1992.
2. P. G. Bruce, *Chem. Commun.* 1817 (1997) and references therein.
3. G. G. Amatucci, J. M. Tarascon, and L.C. Klein, *J. Electrochem. Soc.* **143,** 1114 (1996).
4. T. Ohzuku, A. Ueda, and M. Nagayama, *J. Electrochem. Soc.* **140,** 1862 (1993).

5. T. Nagaura, Paper presented at "4th Int. Rechargeable Battery Seminar," Deerfield Beach, FL. 1990; T. Nagaura and K. Tazawa, *Prog. Batteries Col. Cells* **9,** 20 (1990).
6. K. Mizushima, P. C. Jones, P. J. Wiseman, and J. B. Goodenough, *Mater. Res. Bull.* **15,** 783 (1980).
7. P. G. Bruce, *Philos, Trans. R. Soc. Lond. A* **354,** 1577 (1996).
8. G. Pistoia, Ed., "Lithium Batteries, New Materials, Development and Perspectives," Elsevier Science B.V., Amsterdam, 1994.
9. Y. Gao and J. R. Dahn, *J. Electrochem. Soc.* **143,** 100 (1996).
10. M. M. Thackeray, W. I. F. David, P. G. Bruce, and J. B. Goodenogh, *Mater. Res. Bull.* **18,** 461 (1983).
11. M. M. Thackeray, P. J. Johnson, L. A. de Picciotto, W. I. F. David, P. G. Bruce, and J. B. Goodenough, *Mater. Res. Bull.* **19,** 179 (1984).
12. J. B. Goodenough, M. M. Thackeray, W. I. F. David, and P. G. Bruce, *Rev. Chim. Minér.* **21,** 435 (1984).
13. Japan Electronics, March 6th (1996).
14. J. M. Tarascon, F. Coowar, G. Amatuci, F. K. Shokoohi, and D. G. Guyomard, *J. Power Sources* **54,** 103 (1995).
15. R.J. Gummow, A. de Kock, and M. M. Thackeray, *Solid State Ionics* **69,** 59 (1994).
16. H. Huang and P. G. Bruce, *J. Electrochem. Soc.* **141,** L106 (1994).
17. (a) G. Pistoia, A. Antonni, R. Rosati, and D. Zane, *Electrochim. Acta.* **41,** 2683 (1996); (b) G. Pistoia, D. Zane, and Y. Zhang, *J. Electrochem. Soc.* **142,** 2551 (1995).
18. A. R. Armstrong and P. G. Bruce, *Nature* **381,** 499 (1996).
19. C. Delmas and F. Capitaine, Presented at the 8th Int. Meeting on Lithium Batteries," Nagoya, Japan, 1996.
20. M. Tabuchi, K. Ado, H. Kobayashi, H. Kageyama, C. Masqueler, A. Kondo, and R. Kanno, *J. Electrochem. Soc.* **145,** L49 (1998).
21. A. R. Armstrong, R. L. Gitzendanner, A. D. Robertson, and P. G. Bruce, *Chem. Comm.* **1998,** 1833 (1998).
22. R. I. Smith, S. Hull, and A. R. Armstrong, *Mater. Sci. Forum* **166–169,** 251 (1994).
23. J. C. Matthewman, P. Thompson, and P. J. Brown, *J. Appl. Crystallogr.* **15,** 167 (1982).
24. P. J. Brown and J. C. Matthewman, Rutherford Appleton Laboratory Report, RAL-87-010 (1987).
25. V. F. Sears, *Neutron News* **3,** No. 3, 26 (1992).
26. W. D. Johnston, R. R. Heikes, and D. Sestrich, *J. Phys. Chem. Solids* **7,** 1 (1958).
27. J. N. Reimens, W. Li, E. Rossen, and J. R. Dahn, *Mat. Res. Soc. Symp. Proc.* **293,** 3 (1993).
28. R. J. Gummow, D. C. Liles, and M. M. Thackeray, *Mater. Res. Bull.* **28,** 235 (1993).
29. R. D. Shannon, *Acta Cryst. A* **32,** 751 (1976).
30. P. G. Bruce, A. R. Armstrong, and R. L. Gitzendanner, *J. Mater. Chem.* **9,** 193 (1999).
31. H. Huang and P. G. Bruce, *J. Power Sources* **54,** 52 (1995).